ChemPubSoc Europe

DOI: 10.1002/chem.201504249

CHEMISTRY
A European Journal
Communication

Photoisomerization

Visible-Light-Induced Morphological Changes of Giant Vesicles by Photoisomerization of a Ruthenium Aqua Complex

Masanari Hirahara,*[a] Akira Tsukamoto,[b] Hiroki Goto,[a] Shigeru Tada,[b] Masayuki Yagi,[c] and Yasushi Umemura*[a]

Abstract: Visible- and red-light responsive vesicles were prepared by incorporating a ruthenium aqua complex having two alkyl chains on tridentate and asymmetrical bidentate ligands (*proximal*-**2**: $[Ru(C_{10}tpy)(C_{10}pyqu)OH_2]^{2+}$, $C_{10}tpy$ = 4′-decyloxy-2,2′;6′,2″-terpyridine, $C_{10}pyqu$ = 2-[2′-(6′-decyloxy)-pyridyl]quinoline). The ruthenium complex of *proximal*-**2** with closed alkyl chain geometry and a cylinder-like molecular shape exhibited photoisomerization to *distal*-**2** with an open alkyl chain geometry and a cone-like shape, both in an aqueous solution and in vesicle dispersions. We observed that light irradiation of giant vesicles containing *proximal*-**2** induced diverse morphological changes.

Controlling morphologies of molecular assemblies by external stimuli is an important issue in the development of their numerous applications.[1,2] In particular, structural changes of vesicles through light stimulation are an attractive target in the design of drug delivery systems and chemical reactors.[3–6] Organic photochromic compounds showing *cis–trans* photoisomerization (such as stilbene and azobenzene derivatives) have often been incorporated into molecular assemblies.[5–11] In most cases, UV light has been used to drive morphological changes, but it is well known that irradiation of UV light often induces DNA damage and cell death.[12] Alternatively, the use of visible or near-infrared (NIR) light is attractive because of their high tissue permeability and the availability of abundant sunlight energy. In this context, polypyridyl ruthenium complexes are potential candidates as visible-light-responsive surfactants, because these complexes are thermodynamically stable, and show visible-light-induced ligand substitution[13,14] and photoisomerization,[15–22] which have been recently applied to photoinduced motions of large structures[23,24] Furthermore, these ruthenium complexes have been identified as molecular catalysts[25–29] and bioactive molecules.[30,31] Thus, functionalization of vesicles containing ruthenium complexes will expand their applications as photoreactive vesicles.

Some recent articles have described lipid vesicles incorporating ruthenium complexes with hydrophobic moieties. Koshiyama et al. investigated water oxidation catalysis by a ruthenium complex embedded within vesicles in the dark.[32] Bonnet et al. used the photoinduced ligand substitution reaction to release bioactive ruthenium complexes from vesicles by visible or NIR light irradiation.[33,34] In these studies, however, there were no morphological changes in the vesicles under light irradiation.

We recently reported irreversible[35–38] and reversible photoisomerizations[39] of mononuclear ruthenium aqua complexes having an asymmetric bidentate ligand (Scheme 1). The reversibility of the reaction is controlled by intramolecular hydrogen bonding between the aqua ligand and the pendant moiety of the bidentate ligand.[36]

Herein, we describe the visible-light-induced morphological changes in giant multilamellar vesicles. We synthesized a new series of ruthenium aqua complexes with long alkyl chains on tridentate and/or bidentate ligands for incorporation into vesicles, as shown in Scheme 2. The morphological changes were induced by the molecular photoisomerization of *proximal*-**2** embedded within the vesicles (*proximal*-**2**: $[Ru(C_{10}tpy)(C_{10}pyqu)OH_2]^{2+}$, $C_{10}tpy$ = 4′-decyloxy-2,2′;6′,2″-terpyridine, $C_{10}pyqu$ = 2-[2′-(6′-decyloxy)-pyridyl]-quinoline). We

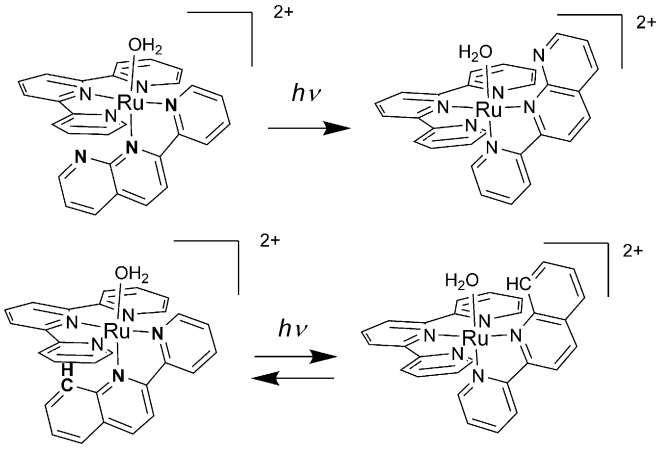

Scheme 1. Irreversible and reversible photoisomerizations of ruthenium aqua complexes.[35,36,39]

[a] *Dr. M. Hirahara, H. Goto, Prof. Y. Umemura*
Department of Applied Chemistry, School of Applied Science
National Defense Academy of Japan
Hashirimizu 1-10-20, Yokosuka, Kanagawa, 239-8686 (Japan)
E-mail: hirahara@nda.ac.jp

[b] *Prof. A. Tsukamoto, S. Tada*
Department of Applied Physics, School of Applied Science
National Defense Academy of Japan (Japan)

[c] *Prof. M. Yagi*
Department of Materials Science and Technology, Faculty of Engineering
Niigata University, 8050 Ikarashi-2, Niigata, 950-2181 (Japan)

Supporting information and ORCID(s) from the author(s) for this article are available on the WWW under http://dx.doi.org/10.1002/chem.201504249.

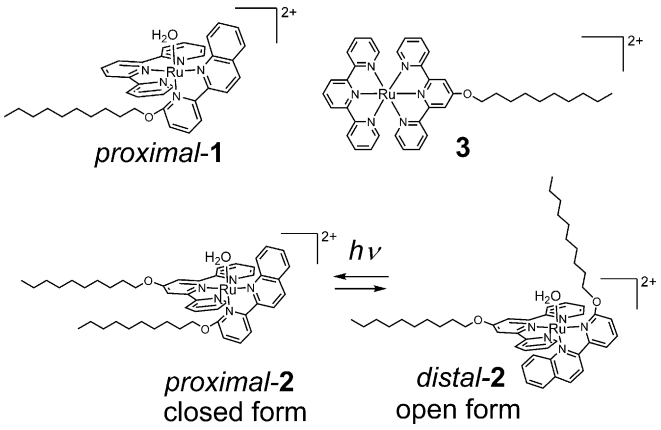

Scheme 2. Ruthenium complexes used in this work, and the photoisomerization equilibrium between *proximal*-**2** and *distal*-**2**.

observed that the morphological changes in vesicles were driven by red light (635 nm), which can permeate mammalian tissues. For comparison, we prepared two kinds of ruthenium complex with a single alkyl chain: *proximal*-**1**; $[Ru(tpy)(C_{10}pyqu)OH_2]^{2+}$ (tpy = 2,2′;6′,2″-terpyridine), and **3**; $[Ru(tpy)(C_{10}tpy)]^{2+}$. Control experiments suggested that photodissociation of the aqua ligand in *proximal*-**2**, followed by geometrical change of the two alkyl chains, was an important factor in driving the morphological changes.

In mixed aqueous solutions, both *proximal*-**1** and *proximal*-**2** showed photoisomerization equilibria with the corresponding *distal* isomers, according to ^{1}H NMR measurements (Figure 1; Supporting Information, Figure S1). The ratio of the *proximal* and *distal* isomers in the photostationary state was 54:46 and 40:60 for complexes **1** and **2**, respectively. The quantum yields for forward and back photoisomerizations for *proximal*- and *distal*-**2** were determined to be 3.7×10^{-3} and 2.5×10^{-3}, respectively, using monochromic light at 508 nm.

Giant vesicles containing ruthenium complexes were prepared by hydration of films containing the ruthenium complexes and phospholipids. The vesicles prepared from *proximal*-**2** and DOPC (abbreviated as *proximal*-**2**/DOPC; DOPC = 1,2-dioleoyl-*sn*-glycero-3-phosphocholine) are shown in Figure 2A,B and the Supporting Information, Figure S2. The average size of the vesicles was 15 μm and giant multilamellar vesicles larger than 50 μm were observed. The dark color of the vesicle in Figure 2B arises from the concentric lipid layers (see below). On the other hand, vesicles prepared from DOPC alone gave multilamellar structures with an average size of 24 μm (Figure 2C; Supporting Information, Figure S3). Vesicles *proximal*-**1**/DOPC and **3**/DOPC are shown in the Supporting Information, Figures S4 and S5, and their average sizes were 20 and 9 μm, respectively.

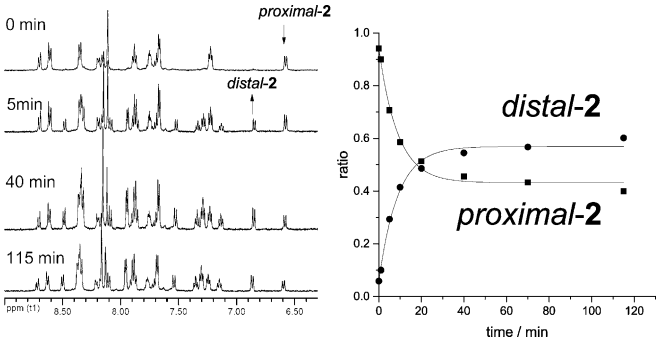

Figure 1. Left: ^{1}H NMR spectra of *proximal*-**2** (1.1 mM) in a mixed aqueous solution (D_2O/CD_3OD/*d*-acetone = 4:2:1) under light irradiation with a 100 W halogen lamp ($\lambda > 380$ nm, 70 mW cm^{-2}). Right: kinetic profiles of *proximal*-**2** (■) and *distal*-**2** (●) under light irradiation, where the ratio of *proximal* and *distal* isomers was estimated from peak areas at 6.59 ppm and 6.87 ppm. The sample solution was prepared by dissolving *proximal*-$[Ru(C_{10}tpy)(C_{10}pyqu)Cl]Cl$ in the mixed solution prior to the measurements.

The absorption spectra for the vesicle dispersions of *proximal*-**2**/DOPC showed an absorption band at 537 nm, which is assigned as metal-to-ligand charge transfer (MLCT) transitions (Supporting Information, Figure S6). The absorption spectra changed slightly under the light irradiation of a 100 W halogen lamp ($\lambda > 380$ nm), with isosbestic points at 276, 303, 435, and 582 nm. The absorbance change at 537 nm was fitted with a single exponential curve. After light irradiation, the vesicle dispersions were evaporated at 45 °C within 5 min, and the product of the photoreaction was checked by ^{1}H NMR spectroscopy (Supporting Information, Figure S7).[40] The formation of the *distal* isomer was confirmed in the spectrum of the vesicle dispersions, similar to the case with photoisomerization in the solution. Thus, photoisomerization of *proximal*-**2** occurred in the vesicles despite the fact that the photoisomerization reaction requires photodissociation of an aqua ligand and re-coordination by a solvent water molecule.[36]

The real-time morphological changes of the giant vesicles were monitored using a digital microscope. For vesicles *proximal*-**2**/DOPC, various morphological changes were observed under visible light irradiation, as depicted in Figure 2. The vesicle in Figure 2A showed increases and decreases in size to give an obscure lamellar structure (see the time courses of size changes in Supporting Information, Figure S9). On the other hand, distortion and budding were observed for the vesicle in Figure 2B. The shape of the vesicle in Figure 2B at 112 min was traced by small granule vesicles (Supporting Information, Figure S10). Vesicles prepared from 10 mol% *proximal*-**2** on DOPC also exhibited various morphological changes, including budding and division into two vesicles (Supporting Information, Figure S11).

We then tested morphological changes of the giant vesicles under red-light irradiation (635 nm). We prepared vesicles containing DOPC, *proximal*-**2**, and rhodamine-DOPC as a fluorescent dye (rhodamine-DOPC:1,2-dioleoyl-*sn*-glycero-3-phosphoethanolamine-*N*-(lissamine rhodamine B sulfonyl). The vesicles in Figure 3A,C displayed fluorescence from their edges, and multilamellar structures were clearly observed from digital microscopy. On the other hand, a dark colored vesicle in Figure 3F displayed fluorescence from interior (Figure 3E), indicating the presence of concentric layers (onion-like structures; see the sliced fluorescence images of vesicles in the Supporting Information, Figures S12 and S13). For vesicles depicted in Figure 3, we observed morphological changes of vesicles

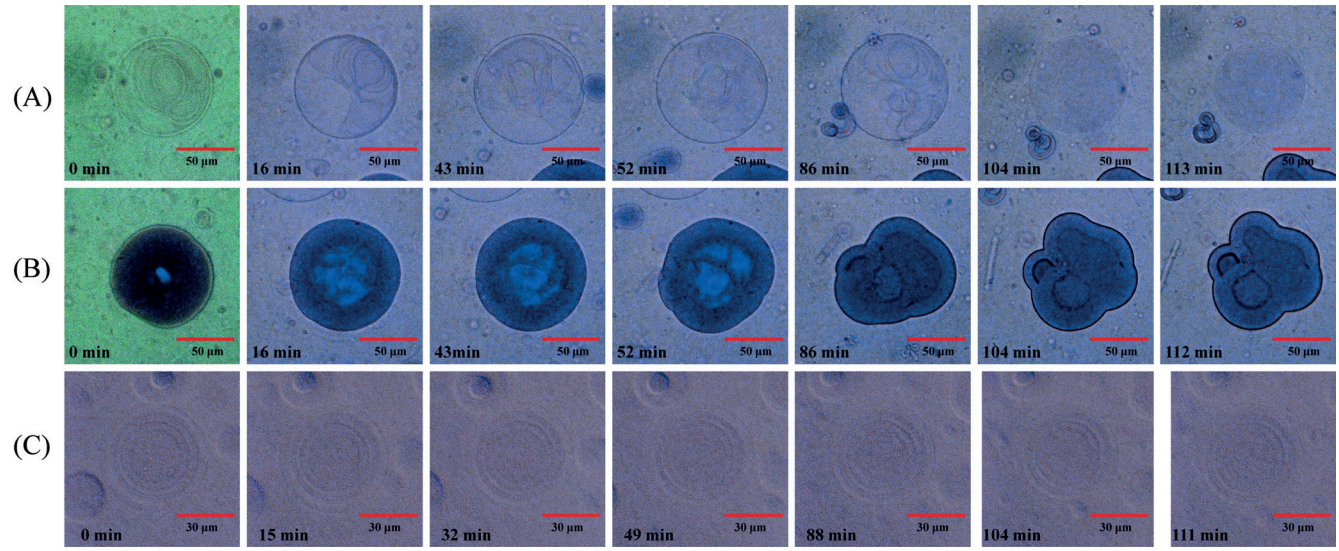

Figure 2. Microscopic images of vesicles under light irradiation with a 100 W halogen lamp ($\lambda > 380$ nm, 120 mW cm^{-2}). A), B): *proximal*-**2**/DOPC (DOPC: 100 nmol, *proximal*-**2**: 20 nmol (20 mol%), water 0.1 mL). C) Vesicles prepared form DOPC alone (DOPC: 100 nmol, water 0.1 mL).

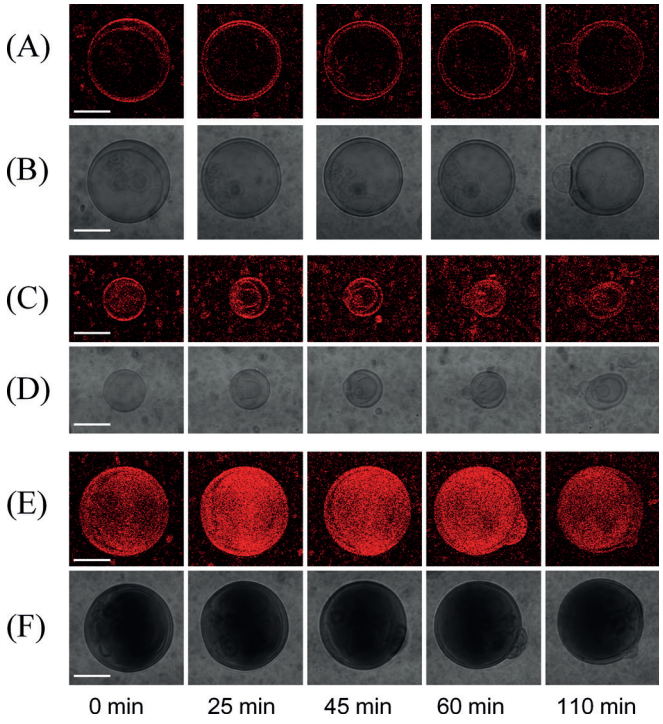

Figure 3. Confocal fluorescence microscopy (A, C, and E), and digital microscopy (B, D, and F) images of giant vesicles containing DOPC (100 nmol), *proximal*-**2** (20 nmol), and rhodamine-DOPC (10 nmol) under irradiation with a diode laser (635 nm, 20 mW). The fluorescence microscopy was measured with excitation at 559 nm. Scale bar: 30 μm.

around 60–110 min under continuous red-light irradiation with a diode laser (635 nm, 20 mW). The vesicle in Figure 3 A, B exhibited budding from the left edge at 110 min. The vesicle in Figure 3 C, D exhibited budding at 60 min and then division and distortion at 110 min. The onion-like vesicle in Figure 3 E also exhibited budding from right edge at 60 min. This is the first example of morphological changes in giant vesicles by light stimuli in the phototherapeutic window (600–1000 nm).

We examined the effect of photodissociation of an aqua ligand on the morphological changes of the vesicles. We earlier reported that photoisomerization reactions were highly suppressed by deprotonation of the aqua ligand (Ru–OH_2 → Ru–OH) because the ruthenium hydroxo complex is inactive towards photoisomerization.[35,36,39] We prepared vesicles containing *proximal*-**2**/DOPC in an aqueous NaOH solution (10 mM), and for comparison, the vesicles were also prepared in 5 mM Na_2SO_4. In the NaOH solution, the MLCT absorption band of the *proximal*-**2**/DOPC displayed a red-shift of 43 nm from that prepared in water or an aqueous solution of 5 mM Na_2SO_4. Under basic conditions, only 10% of vesicles showed size increases, and neither budding nor division of vesicles were observed after light irradiation (Supporting Information, Figure S14). On the other hand, 80% of vesicles *proximal*-**2**/DOPC in 5 mM Na_2SO_4 showed size increases or budding (Supporting Information, Figure S15). These results suggest that photodissociation of the aqua ligand in *proximal*-**2** is essential for the morphological changes in the vesicles. These results furthermore imply that the light induced morphological changes can be controlled by the external environment (pH change).

The percentages of the vesicles showing changes in their morphologies under light irradiation are shown in Figure 4. For *proximal*-**2**/DOPC, the percentages increased as the amount of *proximal*-**2** increased (0–20 mol%). On the other hand, the percentages were lower than 11% for vesicles prepared from DOPC, *proximal*-**1**/DOPC, and **3**/DOPC. Because the absorption spectrum of *proximal*-**2** resembled that of *proximal*-**1** (Supporting Information, Figure S16), the morphological changes of vesicles should not be induced by heating of the vesicle dispersions under light irradiation. The above data suggest that photoisomerization with geometrical change of alkyl chains is a key factor driving the morphological changes.

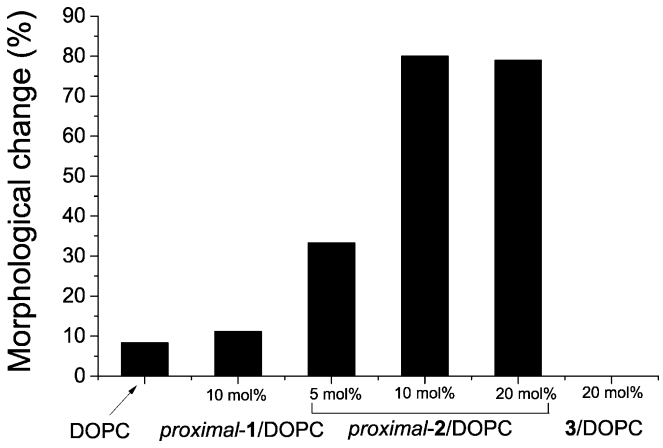

Figure 4. Percentage of vesicles (> 10 μm) showing morphological change after 30 min visible-light irradiation ($\lambda > 380$ nm, 120 mW cm^{-2}). The percentages of the morphological changes were calculated from the results of optical microscopic images.

The morphological changes of *proximal*-**2**/DOPC can be explained by the difference in the molecular shapes of both isomers. The ruthenium complex with a closed alkyl chain geometry, *proximal*-**2**, possesses a cylinder-like molecular shape, with a 1.0 nm head and 1.1 nm tail according to density functional theory (DFT) calculations (Supporting Information, Figure S17), which is similar to that of DOPC.[41,42] The similar molecular shapes of *proximal*-**2** and DOPC would allow the formation of giant multilamellar vesicles under the experimental conditions. On the other hand, *distal*-**2** possesses a cone-like structure with a 1.1 nm head and 2.6 nm tail. The mixing of cylinder-like and cone-like surfactants can induce membrane stress and the transition of lamella into a nonlamellar phase.[41,42] We speculated that formation of *distal*-**2** can cause membrane stress in the bilayer structures.

To examine the membrane stress caused by the formation of *distal*-**2**, we prepared vesicles from lipid films containing DOPC and both *proximal*-**2** and *distal*-**2**. The size and morphology of the vesicles (*proximal*-**2** and *distal*-**2**)/DOPC (Supporting Information, Figure S18) were quite different from those prepared from *proximal*-**2**/DOPC (Supporting Information, Figure S2). Most of vesicles were smaller than 5 μm, and vesicles larger than 15 μm were not observed. Thread-like vesicles were found on their morphologies, which were not seen in *proximal*-**2**/DOPC vesicles before light irradiation. These thread-like vesicles were often found after photoirradiation of *proximal*-**2**/DOPC vesicles (Supporting Information, Figure S10). We therefore consider that photoisomerization to *distal*-**2** in the bilayer induces membrane stress and morphological changes of giant vesicles.

In conclusion, we have prepared a ruthenium aqua complex, *proximal*-**2**, that shows photoisomerization in vesicle dispersions. Visible light irradiation of the vesicles containing *proximal*-**2** induced diverse morphological changes. The morphological changes were driven by the use of red light (635 nm), which lies within the phototherapeutic window.

Acknowledgements

The authors thank Prof. Yoshinobu Yokomori, Prof. Koji Nishi, and Dr. Natsumi Kamiya (National Defense Academy of Japan) for kindly supplying a digital microscope (Keyence VHX 5000).

Keywords: aqua complexes · morphology · photoisomerization · ruthenium · vesicles

[1] A. Natansohn, P. Rochon, *Chem. Rev.* **2002**, *102*, 4139 – 4176.
[2] S. Yagai, A. Kitamura, *Chem. Soc. Rev.* **2008**, *37*, 1520 – 1529.
[3] P. Shum, J.-M. Kim, D. H. Thompson, *Adv. Drug Delivery Rev.* **2001**, *53*, 273 – 284.
[4] D. M. Vriezema, M. Comellas Aragonès, J. A. A. W. Elemans, J. J. L. M. Cornelissen, A. E. Rowan, R. J. M. Nolte, *Chem. Rev.* **2005**, *105*, 1445 – 1490.
[5] E. Mabrouk, D. Cuvelier, F. Brochard-Wyart, P. Nassoy, M.-H. Li, *Proc. Natl. Acad. Sci. USA* **2009**, *106*, 7294 – 7298.
[6] X. Song, J. Perlstein, D. G. Whitten, *J. Am. Chem. Soc.* **1997**, *119*, 9144 – 9159.
[7] T. Hamada, Y. T. Sato, K. Yoshikawa, T. Nagasaki, *Langmuir* **2005**, *21*, 7626 – 7628.
[8] A. Diguet, M. Yanagisawa, Y.-J. Liu, E. Brun, S. Abadie, S. Rudiuk, D. Baigl, *J. Am. Chem. Soc.* **2012**, *134*, 4898 – 4904.
[9] T. Hamada, R. Sugimoto, M. d. C. Vestergaard, T. Nagasaki, M. Takagi, *J. Am. Chem. Soc.* **2010**, *132*, 10528 – 10532.
[10] L. Li, M. Rosenthal, H. Zhang, J. J. Hernandez, M. Drechsler, K. H. Phan, S. Rütten, X. Zhu, D. A. Ivanov, M. Möller, *Angew. Chem. Int. Ed.* **2012**, *51*, 11616 – 11619; *Angew. Chem.* **2012**, *124*, 11784 – 11787.
[11] K. Ishii, T. Hamada, M. Hatakeyama, R. Sugimoto, T. Nagasaki, M. Takagi, *ChemBioChem* **2009**, *10*, 251 – 256.
[12] B. Alberts, A. Johnson, J. Lewis, M. Raff, K. Roberts, P. Walter, *Molecular Biology of the Cell*, 4th edition, Garland Science, New York, **2002**.
[13] D. V. Pinnick, B. Durham, *Inorg. Chem.* **1984**, *23*, 1440 – 1445.
[14] J. J. Rack, J. R. Winkler, H. B. Gray, *J. Am. Chem. Soc.* **2001**, *123*, 2432 – 2433.
[15] B. Durham, S. R. Wilson, D. J. Hodgson, T. J. Meyer, *J. Am. Chem. Soc.* **1980**, *102*, 600 – 607.
[16] S. Bonnet, J.-P. Collin, J.-P. Sauvage, *Inorg. Chem.* **2006**, *45*, 4024 – 4034.
[17] S. Bonnet, J.-P. Collin, J.-P. Sauvage, *Inorg. Chem.* **2007**, *46*, 10520 – 10533.
[18] S. Miyazaki, T. Kojima, S. Fukuzumi, *J. Am. Chem. Soc.* **2008**, *130*, 1556 – 1557.
[19] S. K. Padhi, R. Fukuda, M. Ehara, K. Tanaka, *Inorg. Chem.* **2012**, *51*, 5386 – 5392.
[20] A. W. King, L. Wang, J. J. Rack, *Acc. Chem. Res.* **2015**, *48*, 1115 – 1122.
[21] S. J. Wezenberg, K.-Y. Chen, B. L. Feringa, *Angew. Chem. Int. Ed.* **2015**, *54*, 11457 – 11461; *Angew. Chem.* **2015**, .
[22] B. A. Albani, C. B. Durr, B. Pena, K. R. Dunbar, C. Turro, *Dalton Trans.* **2014**, *43*, 17828 – 17837.
[23] Y. Jin, S. I. M. Paris, J. J. Rack, *Adv. Mater.* **2011**, *23*, 4312 – 4317.
[24] Y. Jin, D. Harrington, A. A. Rachford, J. J. Rack, *RSC Adv.* **2014**, *4*, 62920 – 62925.
[25] J. J. Concepcion, J. W. Jurss, J. L. Templeton, T. J. Meyer, *J. Am. Chem. Soc.* **2008**, *130*, 16462 – 16463.
[26] L. Duan, F. Bozoglian, S. Mandal, B. Stewart, T. Privalov, A. Llobet, L. Sun, *Nat. Chem.* **2012**, *4*, 418 – 423.
[27] E. Masllorens, M. Rodriguez, I. Romero, A. Roglans, T. Parella, J. Benet-Buchholz, M. Poyatos, A. Llobet, *J. Am. Chem. Soc.* **2006**, *128*, 5306 – 5307.
[28] A. D. Chowdhury, A. Das, I. K, S. M. Mobin, G. K. Lahiri, *Inorg. Chem.* **2011**, *50*, 1775 – 1785.
[29] J. L. Boyer, D. E. Polyansky, D. J. Szalda, R. Zong, R. P. Thummel, E. Fujita, *Angew. Chem. Int. Ed.* **2011**, *50*, 12600 – 12604; *Angew. Chem.* **2011**, *123*, 12808 – 12812.
[30] B. S. Howerton, D. K. Heidary, E. C. Glazer, *J. Am. Chem. Soc.* **2012**, *134*, 8324 – 8327.

[31] B. A. Albani, B. Peña, N. A. Leed, N. A. B. G. de Paula, C. Pavani, M. S. Baptista, K. R. Dunbar, C. Turro, *J. Am. Chem. Soc.* **2014**, *136*, 17095 – 17101.
[32] T. Koshiyama, N. Kanda, K. Iwata, M. Honjo, S. Asada, T. Hatae, Y. Tsuji, M. Yoshida, M. Okamura, R. Kuga, S. Masaoka, M. Ohba, *Dalton Trans.* **2015**, *44*, 15126 – 15129.
[33] S. Bonnet, B. Limburg, J. D. Meeldijk, R. J. M. K. Gebbink, J. A. Killian, *J. Am. Chem. Soc.* **2011**, *133*, 252 – 261.
[34] M. Frasconi, Z. Liu, J. Lei, Y. Wu, E. Strekalova, D. Malin, M. W. Ambrogio, X. Chen, Y. Y. Botros, V. L. Cryns, J.-P. Sauvage, J. F. Stoddart, *J. Am. Chem. Soc.* **2013**, *135*, 11603 – 11613.
[35] H. Yamazaki, T. Hakamata, M. Komi, M. Yagi, *J. Am. Chem. Soc.* **2011**, *133*, 8846 – 8849.
[36] M. Hirahara, M. Z. Ertem, M. Komi, H. Yamazaki, C. J. Cramer, M. Yagi, *Inorg. Chem.* **2013**, *52*, 6354 – 6364.
[37] M. Hirahara, S. Nagai, K. Takahashi, K. Saito, T. Yui, M. Yagi, *Inorg. Chem.* **2015**, *54*, 7627 – 7635.
[38] K. Takahashi, X. Zhang, M. Hirahara, T. Sato, K. Saito, T. Yui, M. Yagi, *J. Photochem. Photobiol. A* **2015**, *313*, 117 – 125.
[39] M. Hirahara, H. Tomoya, A. B. League, M. Z. Ertem, K. Takahashi, S. Nagai, K. Inaba, H. Yamazaki, K. Saito, T. Yui, C. J. Cramer, M. Yagi, *Eur. J. Inorg. Chem.* **2015**, 3892 – 3903.
[40] According to the results of variable-temperature NMR experiments, the photoisomerized *distal*-**2** exhibited thermal back-isomerization to *proximal*-**2** at 45 °C (Supporting Information, Figure S8). During the evaporation process (45 °C, 5 min), a few percent of *distal*-**2** were converted to *proximal*-**2**.
[41] J. N. Israelachvili, in *Intermolecular and Surface Forces (Third Edition)* (Ed.: J. N. Israelachvili), Academic Press, San Diego, **2011**, pp. 577 – 616.
[42] V. A. Frolov, A. V. Shnyrova, J. Zimmerberg, *Cold Spring Harbor Perspect. Biol.* **2011**, *3*, a004747.

Received: October 21, 2015
Revised: November 27, 2015
Published online on January 25, 2016